

Study on a New Vehicle Mounted Isolator with NSSM and CRSM

Chunyu WEI^{a,1} and Xiangyun PANG^a

^aShenyang Jianzhu university, Shenyang, China

Abstract. The zero-stiffness structure has excellent vibration attenuation performance. A new vehicle mounted isolator with negative stiffness spring mechanism (NSSM) and cam-roller spring mechanism (CRSM) is proposed. It has quasi-zero stiffness (QZS) in a small range centered on the initial equilibrium position. Even if the external excitation is strong, this isolator can still maintain stability, and the performance of low dynamic stiffness is not weakened. This characteristic makes the isolator particularly suitable for the vehicle mounted situation. For the harmonic input, the analytical solution of the sprung mass acceleration of the isolator is solved in the time domain. It is concluded that the RMS value and the maximum value of the isolated mass acceleration are proportional to the amplitude of the excitation input. The simulation is carried out and the results show that the theoretical analysis is correct. It also shows that CRMS can effectively suppress the influence of external disturbance without reducing the performance of NSSM, and greatly improve the anti-interference ability of the isolator.

Keywords. QZS, Vibration isolator, NSSM, CRSM, Vehicle mounted

1. Introduction

The QZS isolator has a negative stiffness spring mechanism (NSSM), and the stiffness of the whole system is high-static-low-dynamic (HSLD), so it has a good vibration isolation effect. Recently, the research on QZS vibration isolators has been deepened, and a large number of research results have been achieved [1-3]. The research of vibration isolators mainly includes two aspects: structure and control. The former refers to passive vibration isolators based on new structures and their performance analysis, while the latter refers to vibration isolators with control strategies and their performance research. The passive vibration isolator has no actuator and no control algorithm, so it has low cost and good reliability. Zhao et al. [4] added two pairs of tilted springs to the vibration isolator, and achieved the purpose of reducing the static deflection and increasing the vibration isolation frequency band through ingenious support point design. Traditional QZS isolators often have poor performance if the excitation is large. For this, Wen et al. [5] proposed a method to improve the vibration isolation performance by using a shear-thinning viscous damper. In order to improve the static bearing capacity of the QZS isolator, Katlego et al. [6] designed a vibration absorber which has a negative-stiffness spring between the sprung mass and the base. In some cases, due to space constraints, small vibration isolators are required.

¹ Corresponding Author, WEI Chunyu, Shenyang Jianzhu university; E-mail: weiyu001@163.com.

Therefore, Wang et al. [7] designed a very small QZS isolator by using magnetic rings and a wave-spring at the same time. Inspired by the good attenuation effect of human spine on vibration, Jin et al. [8] proposed a new QZS vibration isolator with bionic human spine structure. It has multi-level negative stiffness structure. In order to obtain nonlinear damping characteristics for different frequency bands, Dong et al. [9] designed a geometric nonlinear damping applied to the vibration isolator, and good performances are attained under the high-frequency input of the base. Due to the low-frequency disturbance of heavy machinery, Gao et al. [10] proposed a new QZS oil-gas isolator, and it uses a corrugated pipe structure as an elastic element and pressurized gas and incompressible liquid as working media. In order to improve the vibration isolation effect at ultra-low frequency, Wang et al. [11] proposed a novel nonlinear vibration isolator with double QZS mechanism by paralleling two different QZS mechanisms with vertical springs. Solaiahari et al. [12] applied fluidic actuators and the helical coil spring into the isolator. Considering the influence of temperature on the structure, Djuitchou et al. [13] designed the auxiliary system for QZS vibration isolator. Zhou et al. [14] designed a novel QZS isolator, which includes V-shaped lever, plate spring and cross-shaped. Kim et al. [15] designed a new QZS vibration isolator for ultra precision testing system, which consists of a pre-tensioned vertical spring and eight horizontal plate springs. The above research on vibration isolators mainly focuses on structural innovation. Good structures can greatly improve the performance of isolators. At present, how to improve the static bearing capacity and the performance under high-frequency excitation is still a research hotspot, and it is also a difficulty in the design of QZS vibration isolators.

In fact, if the QZS vibration isolator can make different sprung masses correspond to different initial equilibrium positions through rapid adjustment, the static bearing capacity only depends on the main spring's stiffness, and there is no problem in theory. However, after the original balance position of the isolator is determined according to the sprung mass, the isolator will be very easy to lose stability when the sprung mass is disturbed by the external excitation. The QZS isolator also has the problem of instability for low-frequency large amplitude excitation. To overcome the above problems, a novel isolator with NSSM and CRSM is proposed in this paper, and the combination of them is the main innovation. The theoretical analysis and simulation research are carried out and the new structure exhibits more excellent vibration isolation performance. In many cases, some precise equipments or patients need to be protected during transportation, and the vehicle mounted vibration isolator can greatly reduce vibration and provide protection. In this paper, a new isolator is proposed for this situation and it can resist large amplitude excitation.

2. Design of the isolator with NSSM and CRSM

The model of the designed isolator is shown in Fig. 1. In this figure, the overall structure of the isolator is symmetrical on both sides, and each side has a NSSM and a CRSM. The hinge of the NSSM is fixedly connected with the outer sleeve of the CRSM. They can slide up and down freely relative to the side wall of the base. The side wall of the base is marked with scales. Before placing the object m , the moving platform compresses the main spring in the vertical direction for a certain distance due to its own gravity to reach a balanced state. At this time, adjust the connecting rod to make it horizontal, and the scale of the base side wall corresponding to the hinge seat is

zero. After placing the object m , calculate the compression amount according to its gravity and the main spring's stiffness, and then adjust the position of the hinge seat to the corresponding scale (EPn), and then lock it. The state at this time is the same as that in Fig. 1. The CRSM can eliminate the influence of adjustment error and external disturbance and avoid system instability.

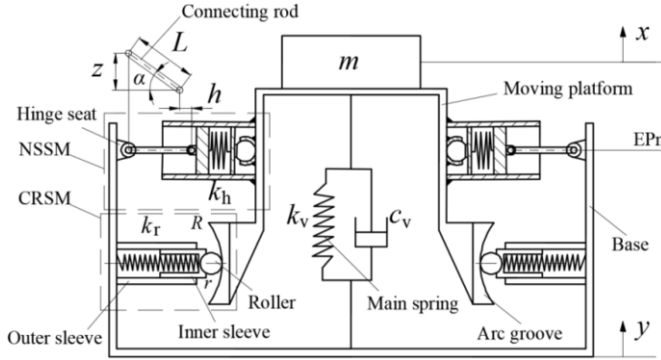


Figure 1. Vibration isolator model.

In Fig. 1, the spring stiffness of the NSSM is k_h , and the length of the connecting rod is L . The main spring's stiffness and damping is k_v and c_v , respectively. x is the mass's displacement from the EPn and y is the base's displacement. k_r is the spring stiffness of the CRSM, r is the radius of the roller and R is the radius of the arc groove.

According to Fig. 1, if the base moves upward z relative to the sprung mass m , the spring compression of the NSSM will be reduced by h (the spring is still in compression). It is assumed that the spring of the CRSM is in the original length state at the initial position. Therefore, the resultant force on the sprung mass m is as follows (ignore the mass of other lightweight components):

$$F = k_v z - 2k_h (\Delta_{\max} - h) \tan \alpha + 2k_r (R - r)(\tan \beta - \sin \beta) \tag{1}$$

where $z = y - x$, $h = L - \sqrt{L^2 - z^2}$, $\tan \alpha = z / \sqrt{L^2 - z^2}$, $\tan \beta = z / \sqrt{(R - r)^2 - z^2}$, $\sin \beta = z / (R - r)$, and Δ_{\max} is the maximum compression of the NSSM spring at the initial state of EPn.

Further, the stiffness of the system can be obtained as follows:

$$k = k_v - 2k_h + 2k_h \frac{L - \Delta_{\max}}{\sqrt{L^2 - z^2}} + 2k_r \left(\frac{R - r}{\sqrt{(R - r)^2 - z^2}} - 1 \right) \tag{2}$$

Eq. (2) shows that when $k_v = 2k_h$ and $L = \Delta_{\max}$, the stiffness of the system mainly depends on the structural parameters of CRSM. There is no correlation between the maximum compression Δ_{\max} and other structural dimensions. Hence, Δ_{\max} can be equal to the length of the connecting rod L . Further, when the roller moves slightly relative to the arc groove, its motion trajectory is similar to a straight line, this means that in this local range $R \rightarrow \infty$. Therefore, according to Eq. (2), we can get:

$$\lim_{R \rightarrow \infty} k \Big|_{\substack{k_v=2k_h \\ \Delta_{\max}=L}} = 0 \tag{3}$$

Eqs. (2) and (3) show that the novel isolator given in Fig. 1 has excellent performance. In a small range centered on the initial equilibrium position, the system has quasi-zero stiffness. In a larger range, it has good stability. Eq. (2) can be modified as follows:

$$k \Big|_{\substack{k_v=2k_h \\ L=\Delta_{\max}}} = 2k_r \left(\frac{1}{\sqrt{1 - \left(\frac{z}{R-r}\right)^2}} - 1 \right) \tag{4}$$

Eq. (4) can be transformed into the non-dimensional form:

$$\bar{k} \Big|_{\substack{k_v=2k_h \\ L=\Delta_{\max}}} = 2 \left(\frac{1}{\sqrt{1 - \bar{z}^2}} - 1 \right) \tag{5}$$

where $\bar{k} = \frac{k}{k_r}$, $\bar{z} = \frac{z}{R-r}$, $|\bar{z}| \in [0,1)$.

For NSSM, z should be less than L , and according to Eq. (5), for simplicity, we can make:

$$L = R - r \tag{6}$$

3. Theoretical analysis of the isolator

According to the structure of the novel isolator, the dynamic equation can be obtained as follows:

$$m\ddot{x} = 2k_r z \left(\frac{R-r}{\sqrt{(R-r)^2 - z^2}} - 1 \right) + C_v \dot{z} \tag{7}$$

When z is small ($z \ll R-r$), Eq. (7) can be simplified as:

$$m\ddot{x} + C_v \dot{x} = C_v \dot{y} \tag{8}$$

When analyzing the isolation performance, the form of base excitation often adopts the cosine function [16]. Therefore, the differential of basic excitation can be taken as:

$$\dot{y} = A \cos \omega t \tag{9}$$

Where A is the amplitude and ω is the angular frequency of the signal respectively.

In terms of Eqs. (8) and (9), a second-order non-homogeneous differential equation can be obtained. Further combined with the initial conditions, the analytical solution of the differential equation can be obtained, as follows:

$$x = \frac{C_v^2 A \sin \omega t - C_v A m \omega \cos \omega t}{\omega(C_v^2 + m^2 \omega^2)} + \frac{A C_v m \cdot e^{-\frac{C_v t}{m}}}{C_v^2 + m^2 \omega^2} \quad (10)$$

Then we can obtain:

$$\ddot{x} = \frac{C_v^3 A e^{-\frac{C_v t}{m}}}{m(C_v^2 + m^2 \omega^2)} - \frac{C_v^2 A \omega \sin \omega t - C_v A m \omega^2 \sin \omega t}{C_v^2 + m^2 \omega^2} \quad (11)$$

The mean value of time from 0 to T is as follows:

$$\bar{\ddot{x}} \stackrel{def}{=} \frac{1}{T} \int_0^T \ddot{x} dt = \frac{A C_v^2 \cos \omega T + A C_v m \omega \sin \omega T - A C_v^2 \cdot e^{-\frac{C_v T}{m}}}{T(C_v^2 + m^2 \omega^2)} \quad (12)$$

Since the vibration level of a signal can be well quantified with its root mean square (RMS) value, and the RMS value of the output acceleration signal can be solved by the following equation:

$$a_{\text{RMS}} = \sqrt{\frac{1}{T} \int_0^T (\ddot{x} - \bar{\ddot{x}})^2 dt} = \frac{A C_v}{T(C_v^2 + m^2 \omega^2)} f(C_v, T, m, \omega) \quad (13)$$

where $f(C_v, T, m, \omega)$ is an expression containing C_v , T , m and ω , and because the complete form of it is too complex, it is omitted.

According to Eq. (11), the ratio of the maximum value of the acceleration output of the sprung mass m to the amplitude of the input signal is:

$$\lambda_1 = \frac{C_v \omega \sqrt{C_v^2 + m^2 \omega^2}}{C_v^2 + m^2 \omega^2} \quad (14)$$

Similarly, according to Eq. (13), the ratio of the RMS of the acceleration of the isolated mass m to the amplitude of the input signal is:

$$\lambda_2 = \frac{C_v}{T(C_v^2 + m^2 \omega^2)} f(C_v, T, m, \omega) \quad (15)$$

Eqs. (14) and (15) show that when the system parameters and the angular frequency of the excitation signal remain unchanged, the maximum and RMS values of the output acceleration of the sprung mass m are proportional to the amplitude of the excitation signal. This conclusion is extremely important, which is of great significance for predicting and controlling the vibration of the system.

4. Numerical simulations

The performance of the isolator for vehicle is simulated to test the effect of vibration. The parameters are shown in Table 1.

Table 1. Parameters of the Isolator

| Parameter | Value | Parameter | Value |
|-----------|------------|----------------|-------------|
| m | 960 kg | L | 120 mm |
| k_v | 42,000 N/m | c_v | 2,000 N*s/m |
| k_h | 21,000 N/m | Δ_{max} | 120 mm |
| k_r | 10,000 N/m | R | 140 mm |
| r | 20 mm | | |

To protect important devices from damage caused by vibration during transportation and the base of isolators need to be fixed on the vehicle body. Therefore, the typical road excitation is selected as the input of the vibration isolator and the equation is as follow:

$$y = \begin{cases} \frac{h}{2}(1 - \cos(\frac{2\pi V}{l_0}t)), & 0 \leq t \leq \frac{l_0}{V} \\ 0, & t > \frac{l_0}{V} \end{cases} \tag{16}$$

where h and l_0 stand for the height and length of the bump, and $h = 0.02$ m, $l_0 = 2.0$ m, $V = 10$ km/h are chosen in the simulations.

For this isolator, the comparison of three vertical acceleration curves of sprung mass m is shown in Fig. 2. In order to verify the correctness of the conclusion obtained from the above theoretical derivation, make the parameter h in Eq. (16) equal to 0.06 m, and conduct the simulation again. The results are shown in Figs. 3.

It can be seen from Figs. 2 and 3 that the vibration isolator with NSSM and the isolator with CRSM and NSSM have shown excellent performance. However, the difference between them is very small, and CRSM increases the stability of the system and eliminates the possibility of instability. This demonstrates the advantages of combining CRSM and NSSM. While improving stability, CRSM brings minimal side effects, which is the main finding of this paper.

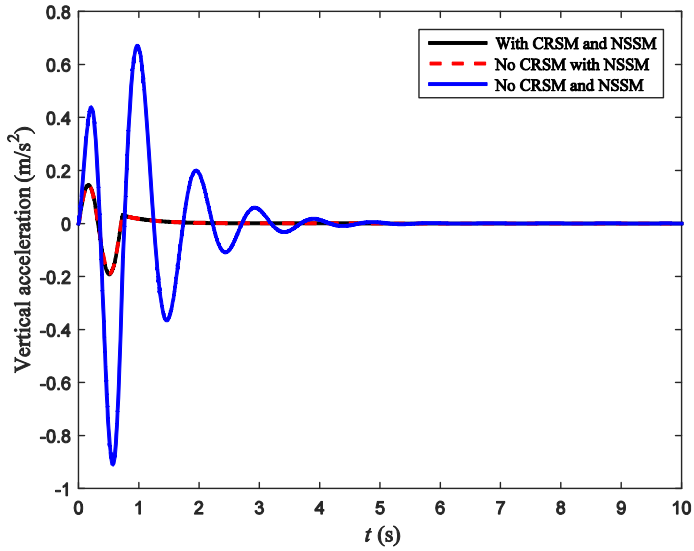


Figure 2. Vertical acceleration curves under case a ($h=0.02$ m).

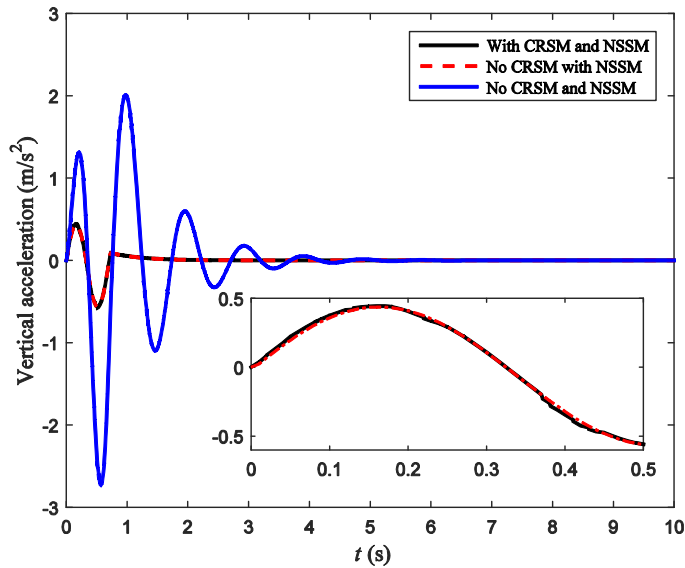


Figure 3. Vertical acceleration curves under case a ($h=0.06$ m).

References

- [1] Chaoran L, Kaiping Y. Design and experimental study of a quasi-zero-stiffness vibration isolator incorporating transverse groove springs. *Archives of Civil and Mechanical Engineering*. 2020 Mar; 20 (3):pp1-21.
- [2] Yue Z, Yufeng M, Zhen W, Chengfei G. Nonlinear low frequency response research for a vibration isolator with quasi-zero stiffness characteristic. *KSCE Journal of Civil Engineering*. 2021 Feb; 25:pp1849-1856.

- [3] Yu H, Gao X. Modeling and stiffness properties for the hydro-pneumatic near-zero frequency vibration isolator with piecewise smooth stiffness. *Journal of Vibration Engineering & Technologies*.2022 Qoc; 10:pp527-539.
- [4] Feng Z, Jinchun J, Quantian L, Shuqian C, Wenliao D. An improved quasi-zero stiffness isolator with two pairs of oblique springs to increase isolation frequency band. *Nonlinear Dynamics*.2021 Mar; 104:pp349-365.
- [5] Guilin W, Yu L, Junfeng H. A quasi-zero-stiffness isolator with a shear-thinning viscous damper. *Applied Mathematics and Mechanics (English Edition)*. 2022 Mar; 43 (3):pp311-326.
- [6] KatlegoT, KuinianL. A passive vibration isolator integrated a dynamic vibration absorber with negative stiffness spring. *Journal of Vibration Engineering & Technologies*. 2022 Oct; 10:pp71-82.
- [7] Qiang W, Jiayi Z, Kai W, Daolin X, Guilin W. Design and experimental study of a compact quasi-zero-stiffness isolator using wave springs. *Science China Technological Sciences*. 2021 Dec; 64:pp2255-2271.
- [8] Guoxin J, Zhenghao W, Tianzhi Y. Cascaded quasi-zero stiffness nonlinear low-frequency vibration isolator inspired by human spine. *Applied mathematics and mechanics-English edition*. 2022 Jun; 43 (6) :pp813-824.
- [9] Guangxu D, Yahong Z, Yajun L, Shilin X, Xinong Z. Enhanced isolation performance of a high-static–low-dynamic stiffness isolator with geometric nonlinear damping. *Nonlinear Dynamics*.2018 Sep; 93 :pp2339-2356.
- [10] Gao X, Teng H. Dynamics and isolation properties for a pneumatic near-zero frequency vibration isolator with nonlinear stiffness and damping. *Nonlinear Dynamics*. 2022 Nov; 102:pp2205-2227.
- [11] Kaizhou Wang, Jiayi C, Yaopeng OY, Huajiang X, Daolin Yang. A nonlinear ultra-low-frequency vibration isolator with dual quasi-zero-stiffness mechanism. *Nonlinear Dynamics*. 2020 Feb; 101:755-773.
- [12] Solaiachari S, Lakshmiopathy J. Analysis of quasi-zero stiffness vibration isolator with fluidic actuators and composite material. *Iranian Journal of Science and Technology, Transactions of Mechanical Engineering* . 2022 Dec; 46:pp863-873.
- [13] DjuitchouTB, MetseboJ, Nana BR, Woafop. Effect of thermal and high static low dynamics stiffness isolator with the auxiliary system on a beam subjected to traffic loads. *Journal of Vibration Engineering & Technologies* . 2022 Sep; 10:pp2021-2032.
- [14] Xinhua Z, Xiao S, Dingxuan Z, Xiao. Y, Kehong Tang. The design and analysis of a novel passive quasi-zero stiffness vibration isolator. *Journal of Vibration Engineering & Technologies*.2021 Sep; 9:pp225-245.
- [15] Jangheon K, Youngjun J, Sangwoo U, Usung P, Soohyun K. A novel passive quasi-zero stiffness isolator for ultra-precision measurement systems. *International Journal of Precision Engineering and Manufacturing*. 2019 Jun; 20:pp1573-1580.
- [16] SuP, JunC, Shuyang L, Jiechang W. Design and analysis of a vibration isolator with adjustable highstatic-low dynamic stiffness. *Iranian Journal of Science and Technology, Transactions of Mechanical Engineering* . 2022 May; 46:pp1195-1207.